machines

MDPI

Article

Fuel Consumption of Backward Vehicle Simulation Following Minimum Fuel Consumption Curve for Optimum Gear Ratios

Ulaş Cankan Çilingiroğlu * and Mehmet İhsan Karamangil

Department of Automotive Engineering, Bursa Uludag University, 16059 Bursa, Turkey; ihsan@uludag.edu.tr
* Correspondence: cilingiroglucankan@uludag.edu.tr

Abstract

Fuel consumption is a critical concern for both environmental and economic reasons. This study proposes a method to operate an engine near the minimum fuel consumption curve by adjusting gear ratios. Using a one-dimensional backward vehicle simulation model, the actual fuel consumption is controlled to follow the desired fuel consumption derived from the Honda Insight fuel conversion map through a proportional–integral–derivative-based approach. Actual fuel consumption, which comes from the driving cycle, and desired consumption, which comes from minimum fuel consumption, are used to determine the optimal gear ratio by supposing that the manual transmission Honda becomes a continuous variable transmission and that gear ratio is a control input for tracking between actual and desired fuel consumption. The minimum fuel consumption curve is obtained from the intersection of constant power and fuel mass flow rate curves. The accuracy of tracking between desired and actual fuel consumption is evaluated across standard driving cycles (New European Driving Cycle, worldwide harmonized light vehicle test procedure Class-3, highway fuel economy test driving, federal test procedure), yielding R^2 values of 0.94, 0.91, 0.88, and 0.91, respectively. These results demonstrate that variable gear ratios can enable operation close to the minimum fuel consumption curve under real driving conditions by considering gearbox dimension limits.

Keywords: driving cycles; minimum fuel consumption curve; fuel conversion efficiency; one-dimensional vehicle model; gear ratio

check for updates

Received: 5 November 2025
Revised: 19 November 2025
Accepted: 24 November 2025
Published: 26 November 2025

Citation: Çilingiroğlu, U.C.; Karamangil, M.İ. Fuel Consumption of Backward Vehicle Simulation Following Minimum Fuel Consumption Curve for Optimum Gear Ratios. *Machines* **2025**, *13*, 1089. https://doi.org/10.3390/machines13121089

Copyright: © 2025 by the authors. Licensee MDPI, Basel, Switzerland. This article is an open access article distributed under the terms and conditions of the Creative Commons Attribution (CC BY) license (https://creativecommons.org/licenses/by/4.0/).

1. Introduction

Reducing fuel consumption is a significant issue due to its environmental effects [1], which include global warming, air pollution, and emissions [2,3], as well as users' economic concerns [4]. To prevent this situation, new regulations such as Euro 2, Euro 4, Euro 6a, Euro 6b, etc., are applied strictly to passenger cars year by year [5,6], and common driving cycles are formed by authorities to predict fuel consumption of vehicles based on different scenarios [7,8].

One example of a vehicle operated on its MFCC is a series hybrid vehicle, in which an internal combustion engine has no mechanical connection to the driveline [9,10]. Automatic/automated transmission also partially eliminates losses when operating vehicles on their MFCC [11], in theory. The effect of the operating engines on MFCC can be observed in a simulation without any automated/automatic transmission. Fuel consumption and emissions are automatically reduced when operating the engines on the MFCC. Several studies have been conducted on the optimization of gear ratios using the energy management system method, which will be presented below. However, these studies primarily

focus on the inner structure of automatic transmissions (CVT, DSG, etc.) [12,13]. Some studies related to defining the most appropriate gear do not provide a clear presentation of obtaining the optimum operating line (minimum fuel consumption curves) [14]. This study focuses solely on optimal gear ratios via PID by reducing complexity and found that the results can be applied to any automatic transmission.

Today, numerous artificial intelligence methods have been successfully applied to address the energy management problem. There are several methods, generally referred to as energy management systems (EMS), that help recover/predict fuel consumption. EMSs are divided into two categories: rule-based and optimization-based methods. For instance, rule-based methods can be applied to online and offline controllers, providing basic and quick calculation time, but they are partially optimal, and a type of rule that is related to the system (non-allowed nonlinear boundary conditions) is applied, which is not the case in optimized-based methods [15]. Fuzzy control carries both the advantages and disadvantages of rule-based methods. Additionally, it requires an expert viewpoint because the rules of control are defined by users based on their experience rather than specific rules [16]. The deterministic rule remains the same, but it is typically applied to the thermovalve and sliding control, utilizing a threshold control strategy [17]. Dynamic programming (DP) is generally used for linear and nonlinear optimization problems, employing a numeric approach to provide the cheapest or optimal trajectory based on the Bellman optimal law independently of initial boundary conditions along with its advantages and disadvantages in optimized-based approaches [18]. However, it is only used as a benchmark to improve real-time applications since it is only used for an offline controller [19].

This study enables the engine to operate at the minimum fuel consumption curve theoretically through the use of an artificial neural network. This obtains a minimum fuel consumption curve and benefit from the intersection of constant power curves and mass flow rate of fuel curves based on the fuel conversion efficiency map of a Honda Insight 1.0 L; additionally, an artificial neural network applied to the minimum fuel consumption curve for giving driving cycles based on engine power, which comes from a 1-D vehicle model.

In previous studies, the method for determining the minimum fuel consumption curve was not clearly defined [11,14]. However, in these previous cases, the first intersection between constant engine power and the mass flow rate of fuel was defined as the minimum fuel consumption. Additionally, constant fuel conversion efficiency values were used instead of dynamic ones, and minimum fuel consumption was derived from numerical equations rather than using meta-modeling methods. This in turn caused missing data representation (not catching some points in the map) [20,21]. The missing data situation is addressed by using an artificial neural network, which is a method of meta-modeling. The reason for selecting an artificial neural network is that it offers greater applicability and accuracy compared to other approaches [18,19], as mentioned above. The most appropriate gear ratios are calculated for the most common driving cycles, which represent real-life road conditions by simplifying the process with PID control.

2. Materials and Methods

2.1. One-Dimensional Model

Analysis of minimum fuel consumption is made real by taking reference of a fuel conversion map of Honda Insight 1.0 L [18] in Simulink software version R2024a with a backward simulation, which is related to the driving cycle without needing any driver inputs; thus, the required engine power is calculated based on the given cycles. The fuel consumption of the backward vehicle simulation model [22] is calculated by considering

the engine powers of driving cycles. Engine power is calculated below the Equation for the 1-D vehicle model [23]:

$$P_{\mathrm{w}} - P_{\mathrm{r}} = P_{\mathrm{a}} \tag{1}$$

If resistance power is expanded, the Equation turns into the following:

$$P_{\mathrm{w}} = P_{(\mathrm{R-F})} + P_{\mathrm{Drag}} + P_{\mathrm{a}} \tag{2}$$

$$P_{\mathrm{w}} = C_{\mathrm{rolling}}\,\mathrm{m} \times \mathrm{ga} \times \cos\alpha \times v_{\mathrm{t}} + 0.5 \times C_{\mathrm{drag}} \times \mathrm{d} \times A_{\mathrm{p}} \times (v_{\mathrm{t}} + v_{\mathrm{w}})^2 \times v_{\mathrm{t}} + m_{\mathrm{ef}} \times \frac{d\mathrm{v}}{d\mathrm{t}} \times v_{\mathrm{t}} \tag{3}$$

$$P_{\mathrm{e}} = \frac{P_{\mathrm{w}}}{\eta \mathrm{a}} \tag{4}$$

In Equation (3), $P_{(\mathrm{R\text{-}F})}$ is the friction resistance power, which comes from the relation between the road and the wheel of a vehicle. P_{drag} is drag resistance power, primarily dependent on the vehicle's shape [24]. Lastly, P_{a} is the resistance power, which is related to the acceleration of a vehicle based on its mass. If acceleration is constant or equal to zero, it will be 0; otherwise, it is changeable based on the performed velocity profile.

On the other hand, in Equation (3), there is an effective mass that is demonstrated as m_{ef} and its calculation is as follows [25]:

$$m_{\mathrm{ef}} = \mathrm{m} \times \mathrm{M} \tag{5}$$

m is the vehicle mass and M is the mass factor. If the mass factor is expanded, then the following is obtained:

$$m_{\mathrm{ef}} = \mathrm{m} \times [1.04 + 0.0025 \times (i_{\mathrm{d}} \times i_{\mathrm{g}})^2] \tag{6}$$

This approach is necessary for vehicle mass, as it is quite sensitive to differential and gear ratios.

The Equation is obtained from a fuel conversion map based on engine power by operating the engine in MFCC for minimum fuel consumption. For backward vehicle simulation's fuel consumption, the Equation is obtained by separating engine power into engine torque and engine radial velocity, Equations (7) and (8). In Section 2.4, both of them will be explained in detail.

$$M_{\mathrm{e}} = \frac{P\mathrm{e} \times R\mathrm{r}}{i\mathrm{d} \times i\mathrm{g} \times v\mathrm{t}} \tag{7}$$

$$\omega_{\mathrm{e}} = \frac{P\mathrm{e}}{M\mathrm{e}} \tag{8}$$

2.2. Driving Cycles

The new European Driving Cycle (NEDC) is a type of cycle composed of two parts: the ECE-15 (Urban Driving Cycle), repeated four times, is plotted from 0 s to 780 s; the EUDC (Extra Urban Driving Cycle) is plotted from 780 s to 1180 s. The distance of NEDC is 11.03 km. ECE-15 is relatively less aggressive and has a lower speed than extra urban driving cycles [26]. NEDC is shown in Figure 1.

However, the NEDC is insufficient for representing fuel consumption in real-life scenarios, so a new driving cycle, known as the Worldwide Harmonized Light Vehicle Test Procedure (WLTP-Class-3), has been developed by authorities with more realistic speed and a suitable profile that reflects real-world driving performance [26]. The total duration of WLTP is 1800 s, and the total distance is 23.27 km. WLTP is shown in Figure 2.

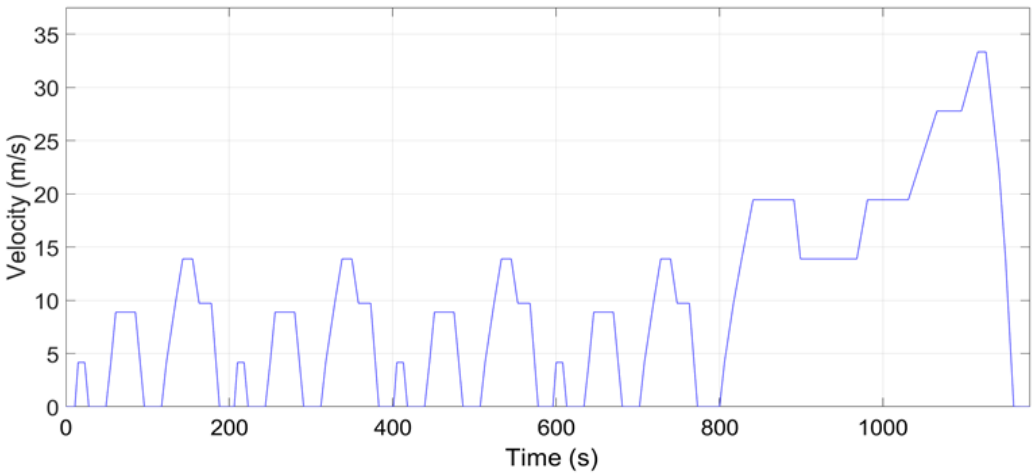


Figure 1. New European Driving Cycle (NEDC).

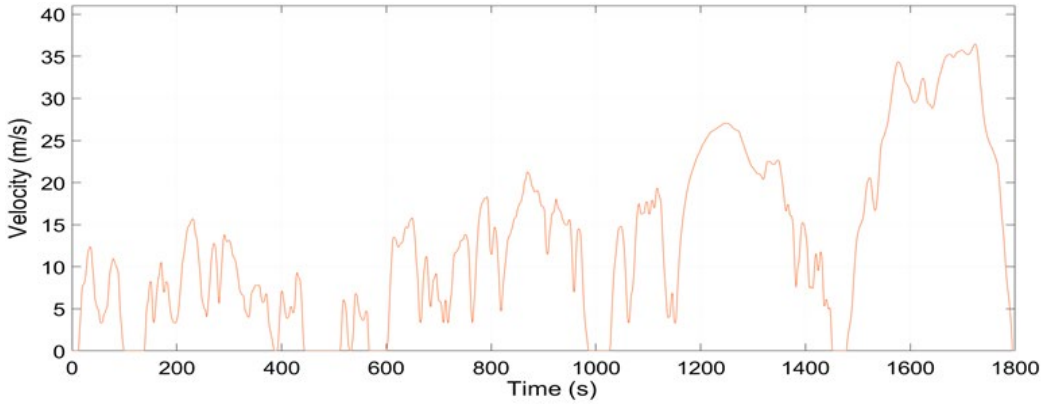


Figure 2. Worldwide harmonized light vehicle test procedure (WLTP-Class-3).

Highway Fuel Economy Driving Schedule (HWFET) is another driving cycle, and one of its significant differences from others is that it drives nonstop until the end of the distance. It was introduced by the EPA (Environmental Protection Agency) for light-duty vehicles [27]. Its total distance is 16.45 km, and its total duration is 765 s. HWFET is shown in Figure 3.

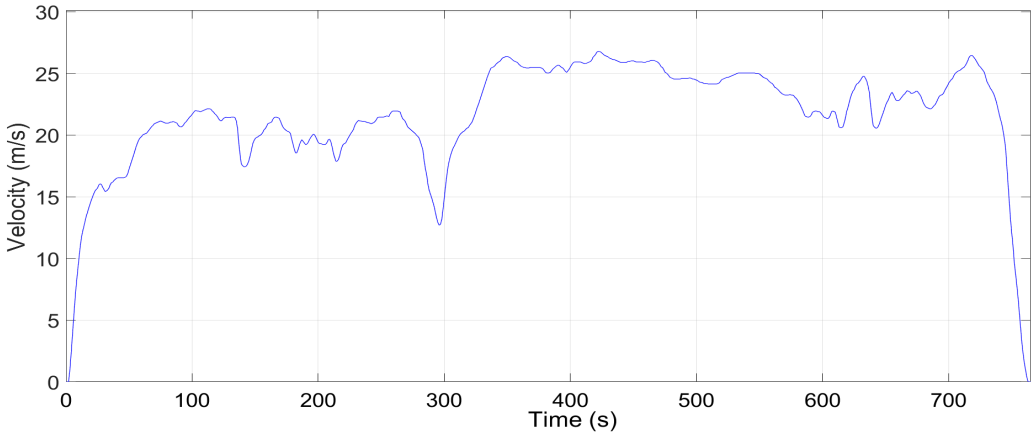


Figure 3. Highway Fuel Economy Driving Schedule (HWFET).

The federal test procedure (FTP-75, without the hot soak phase) is a type of cycle derived from FTP-75 for light-duty vehicles [28]. In the study, the cold start phase, stabilized

phase, and hot start phase are considered, but not the hot soak phase. Its total distance is 17.76 km, and its total duration is 1874 s. FTP-75 is shown in Figure 4.

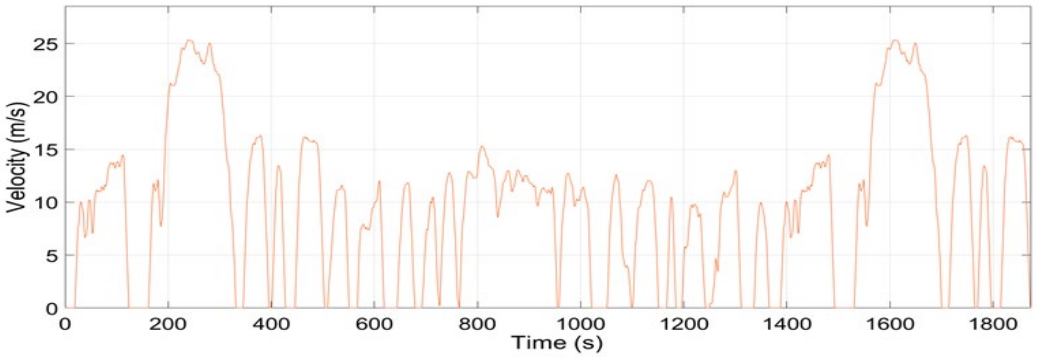


Figure 4. Federal test procedure (FTP-75—without the hot soak phase).

2.3. Vehicle Parameters

Vehicle parameters are related to the Honda Insight 1.0 L engine with a manual gearbox. The parameters can be found in Table 1.

Table 1. Inputs for the calculation of engine power.

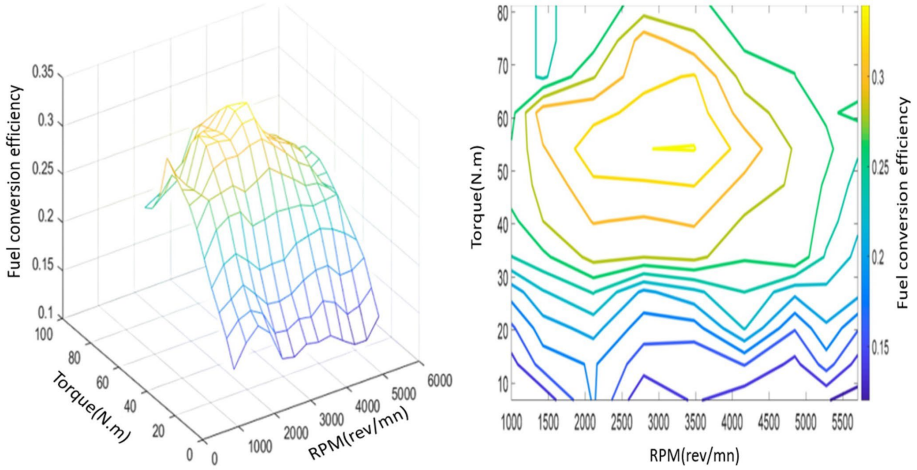
Description	Symbol	Value
Road friction coefficient	$C_{rolling}$	0.015
Gravity acceleration	ga	9.81 m/s^2
Mass	m	1280 kg
Vehicle speed	v_t	Driving cycle
Drag coefficient	C_{drag}	0.335
Projected are	A_p	1.9 m^2
Air density	d	1.225 kg/m^3
Wheel radius	R_r	0.285 m
Differential ratio	i_d	3.21
Powertrain efficiency	η_a	0.9
Gear ratio (Manual)	i_g	i_1 = 3.46 i_2 = 1.75 i_3 = 1.1 i_4 = 0.86 i_5 = 0.71

These gear ratios are for the manual transmission Honda Insight. The vehicle is converted to an automatic transmission by keeping only the differential ratio of the vehicle and finding optimal gear ratios.

2.4. Minimum and Backward Vehicle Simulation's Fuel Consumption

The fuel conversion map of the Honda Insight 1.0 L was used to obtain the minimum fuel consumption curve. Fuel conversion efficiency is a metric that shows the ratio of the brake power produced to the fuel energy applied per cycle. Its maximum achievable efficiency is 34% [21]. Fuel conversion efficiency is related to torque (Nm) and revolutions per minute (rev/min). It is shown in Figure 5 [29].

To specify the minimum fuel consumption, we need a curve that consists of engine power and the mass flow rate of fuel; thus, the minimum fuel consumption can be obtained by the intersection of these two curves. Therefore, the first step is to convert torque and rpm to power.



(**a**) (**b**)

Figure 5. (**a**) The three-dimensional fuel conversion efficiency map of Honda Insight; (**b**) the two-dimensional fuel conversion efficiency map of Honda Insight.

Equation (8) can be written as follows:

$$P_e = M_e \times \omega_e \qquad \text{and to obtain engine speed:} \tag{9}$$

$$P_e = Me \times \frac{2 \times \pi \times ne}{60} \tag{10}$$

Thus, engine power is acquired using torque and engine speed.

In Equations (11) and (12), η_f is fuel conversion efficiency, which comes from Figure 5. Q_{HV} is the fuel's heating value, $\dot{m}_f$ is the fuel's mass flow rate, b_s is the brake-specific fuel consumption, and lastly, P_e is engine power.

$$b_s = \frac{3.6 \times 10^6}{QHV \times \eta f} \tag{11}$$

Therefore, Equation (13) is obtained if Equation (11) is written in Equation (12) and the units of the phenomenon are as follows:

$\dot{m}_f$ (g/s), b_s (g/kWh), P_e (kW) and, Q_{HV} (J/g).

$$\dot{m}_f = \frac{bs \times Pe}{3600} \tag{12}$$

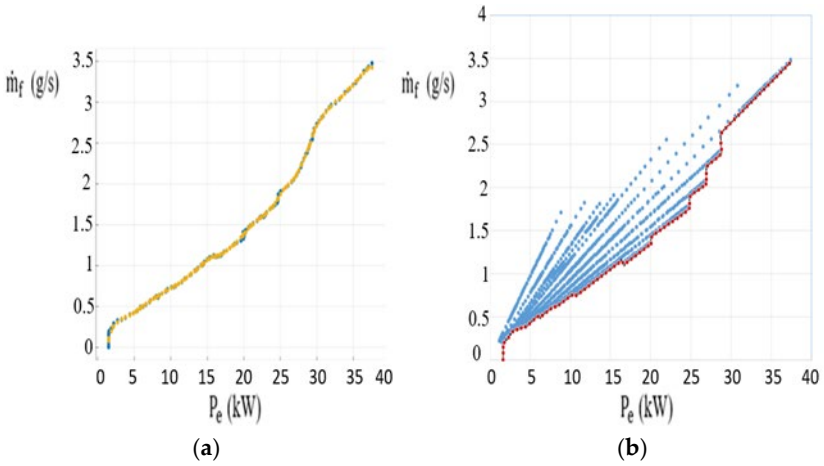
$$\dot{m}_f = \frac{3.6 \times 10^6 \times Pe}{3600 \times QHV \times \eta f} \tag{13}$$

Equation (13) [30] is acquired as a f formula that consists of engine power (P_e) and mass flow rate of fuel ($\dot{m}_f$). The first point of engine power, which touches the mass flow rate of fuel, gives the minimum fuel consumption curve (MFCC). In fact, it is the first intersection between constant power and mass flow rate of fuel (Figure 5, second picture). Q_{HV} is a constant value for gasoline, and its value is 43,000 J/g. P_e is engine power, which comes from the map, and η_f is fuel conversion efficiency.

Equations (7) and (8) benefit the fuel consumption of the backward vehicle simulation. Engine power, is found in Equation (4) based on the driving cycle and is written in Equation (7); in this instance, R_r is the radius of wheel which is constant, v_t is vehicle speed, which comes from driving cycle, i_d is constant based on Table 1, and i_g is the control variable as it is explained in Section 2.5. In Equation (7), the unknown instrument is only i_g, and its value is taken to follow the minimum fuel consumption curve; thus, engine moment (M_e) is calculated, and accordingly, angular velocity (ω_e) is calculated based on Equations

(7) and (8). Fuel conversion efficiency can be found based on Figure 5, along with engine moment, after the angular velocity is converted to engine speed via Equation (10).

Briefly, the minimum fuel consumption (desired fuel consumption) is obtained if the engine's direct parameters (map values) are used in the calculation of Equation (13). The backward vehicle simulation's fuel consumption (actual fuel consumption) is obtained if the specific road condition-driving cycles are used. Figure 6 presents the curve of various levels of fuel consumption. The interpolative method is used to obtain this minimum fuel consumption curve since Figure 6 is obtained by a real engine (fuel conversion map), and it is impossible to exceed these boundary conditions.



(**a**) (**b**)

Figure 6. (**a**) The minimum fuel consumption; (**b**) general fuel consumption.

The most practical way is to examine the R-squared value to ensure the accuracy of the found curve, since it shows how well the model explains the data. Figure 7 demonstrates this confirmation for the minimum fuel consumption curve.

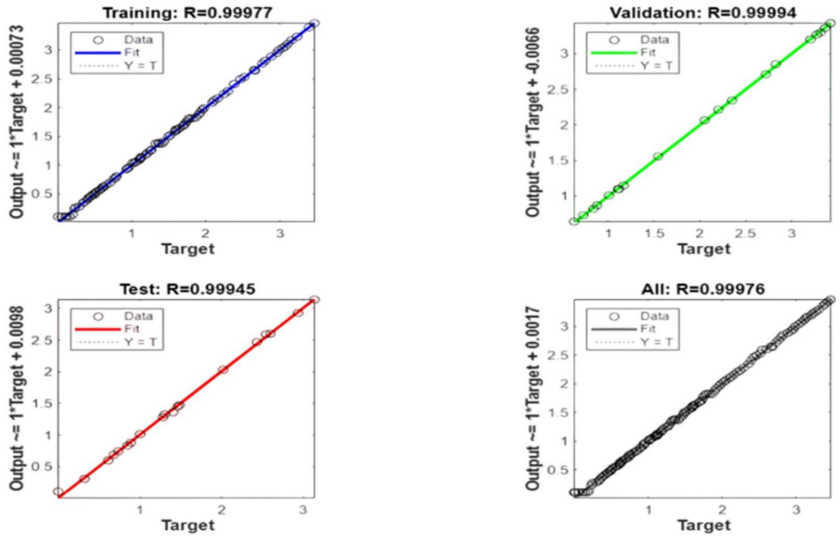


Figure 7. Correlation coefficients for ideal ANNs.

The R-squared value is an approach that compares the actual results with the predicted results. The related formula is presented in Equation (14) [31,32].

$$R^2 = 1 - \frac{\sum_{i=1}^{m}(X_i - Y_i)^2}{\sum_{i=1}^{m}(\overline{Y} - Y_i)^2} \quad (14)$$

$\overline{Y}$ is the mean value of true values (outcome values), X_i is the input variable, and Y_i is the outcome value (true value). Based on this formula, the worst value = $-\infty$ and the best value = +1 are shown.

The minimum fuel consumption is obtained by using the intersection between engine power and mass flow rate of fuel and usage of ANN instead of a numeric formula; thus, accuracy is increased via ANN since numeric formulas are not able to represent complex curves/graphics, etc. The reason for this is that there is no such numerical equation.

2.5. Control Strategy

The control strategy has three main elements. One is the desired fuel consumption related to minimum fuel consumption (Figure 6b). The other two are actual fuel consumption related to the backward vehicle simulation's fuel consumption, based on Equation (13), along with any driving cycle, and the final one is the control signal, which is the gear ratio (i_d) provided to operate the engine on the minimum fuel consumption curve. Actual fuel consumption must follow the desired fuel consumption by arranging a control signal (gear ratio).

In Figure 8, there is a control system subsystem, and inside this system, the engine moment is found based on Equation (7) after the control signal is arranged. After that, the engine radial velocity is determined via the engine moment; thus, the fuel conversion efficiency can be calculated using the engine moment and the engine radial velocity, as obtained from the neural network which is based on the Honda Insight fuel conversion efficiency map, as shown in Figure 9a. Finally, the fuel consumption of the backward vehicle simulation is calculated using Equation (13).

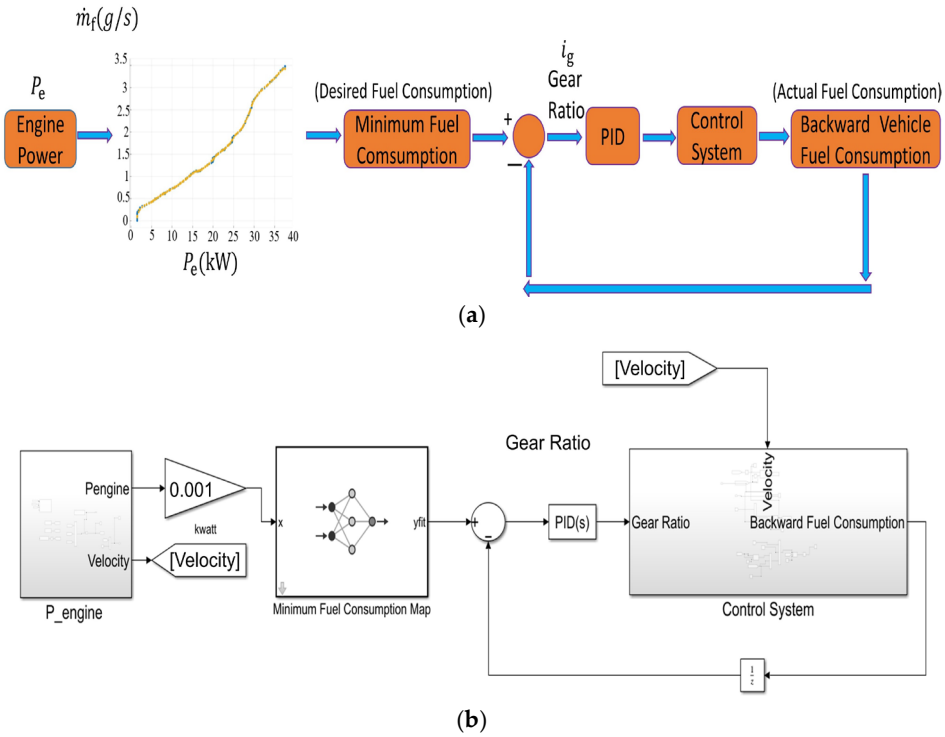
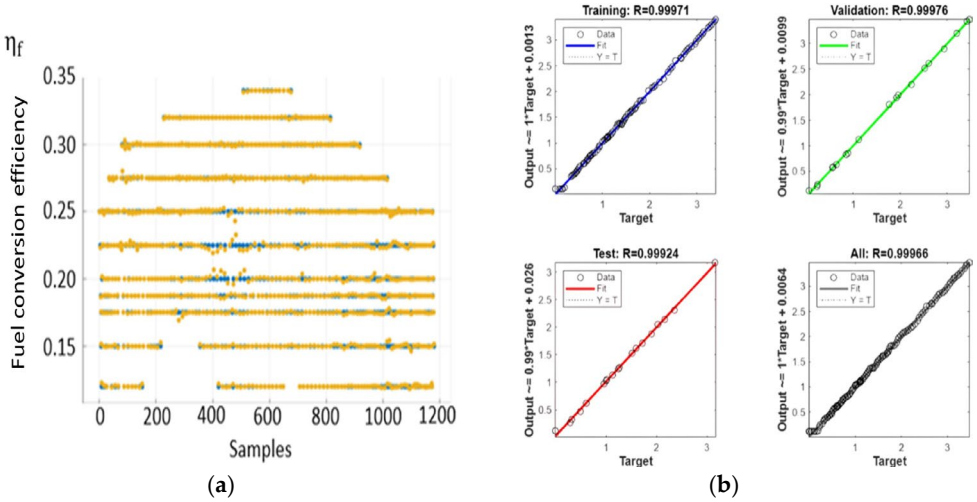


Figure 8. (**a**) Overview of control strategy; (**b**) Simulink model of control strategy.



(**a**) (**b**)

Figure 9. (**a**) The accuracy of the fuel conversion map; (**b**) correlation coefficients for the ideal ANN.

The neural network is applied to Figure 5 to obtain fuel conversion efficiency based on the engine moment and radial velocity inputs. In Figure 9, interpolative Gaussian process regression is used to represent the fuel conversion efficiency map. The reason an interpolative method is used is that it is impossible to exceed these variables, since they are obtained from real engines.

In Figure 9, a discontinuous part is observed below a fuel conversion efficiency value of 0.15, as indicated in the picture on the right in Figure 5. These discontinuities are part of the nature of the fuel conversion efficiency map (Figure 5). This discontinuity is a dead band, which is demonstrated in Figure 5b.

3. Results and Discussion

The obtained $\dot{m}_f$ (g/s) mass flow rate of fuel is converted to liters/100 km by using the Simpson 1/3 method based on the cycle time for both the minimum fuel consumption (desired one) and the backward vehicle simulation's fuel consumption (actual one). Equation (15) is given below:

$$\text{L/100 km} = m_f \times \frac{1}{\text{DR}} \times \frac{1}{d_f} \times 100 \tag{15}$$

m_f (g) is fuel consumption, which comes from the Simpson 1/3 method, DR is the distance of the related driving cycle, d_f is the density of gasoline, and 100 is the conversion coefficient for 100 km. These are presented in Table 2.

Table 2. R-squared values and fuel consumption based on driving cycles.

	HWFET	WLTP	NEDC	FTP-75
Fuel consumption (L/100 km)	3.34	5.10	4.33	4.65
R-squared value	0.88	0.91	0.94	0.91

Table 2 demonstrates how much "backward vehicle simulation's fuel consumption" (actual one) can track the "minimum fuel consumption" (desired one). If the R-squared value equals one, it indicates 100% tracking. This tracking can be observed in Figures 10–13. Naturally, the expectation is that actual fuel consumption exceeds the desired one, as the latter represents the ideal situation.

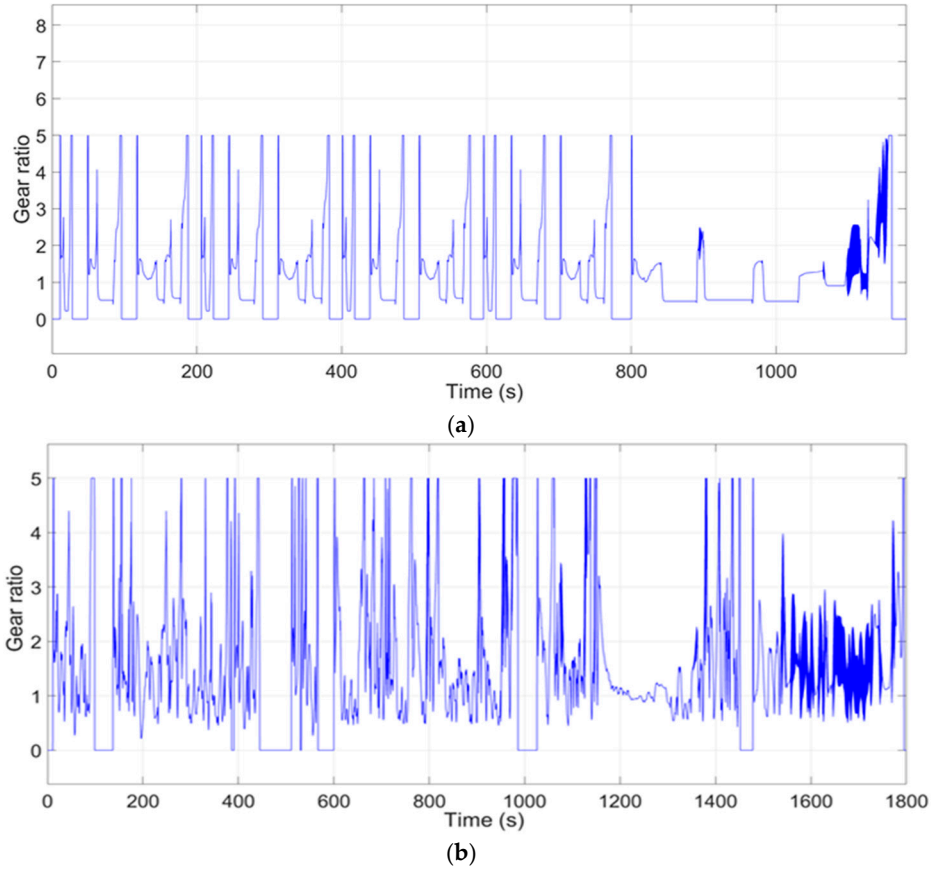


Figure 10. (**a**) Gear ratio rates for NEDC; (**b**) gear ratio rates for WLTP.

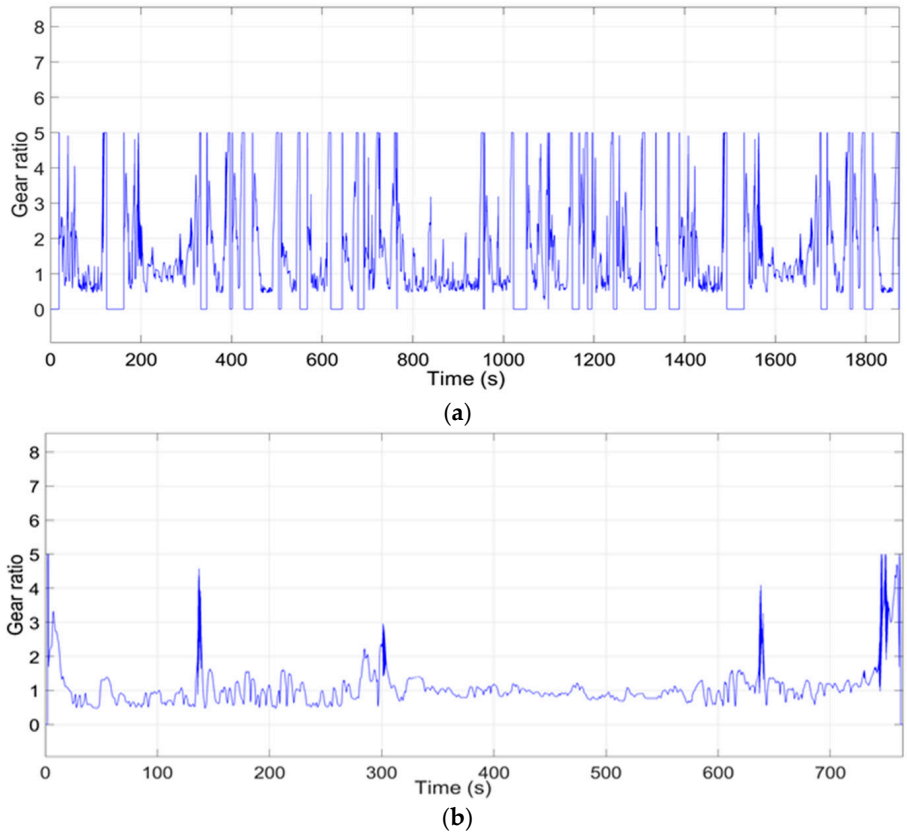


Figure 11. (**a**) Gear ratio rates for FTP-75; (**b**) gear ratio rates for HWFET.

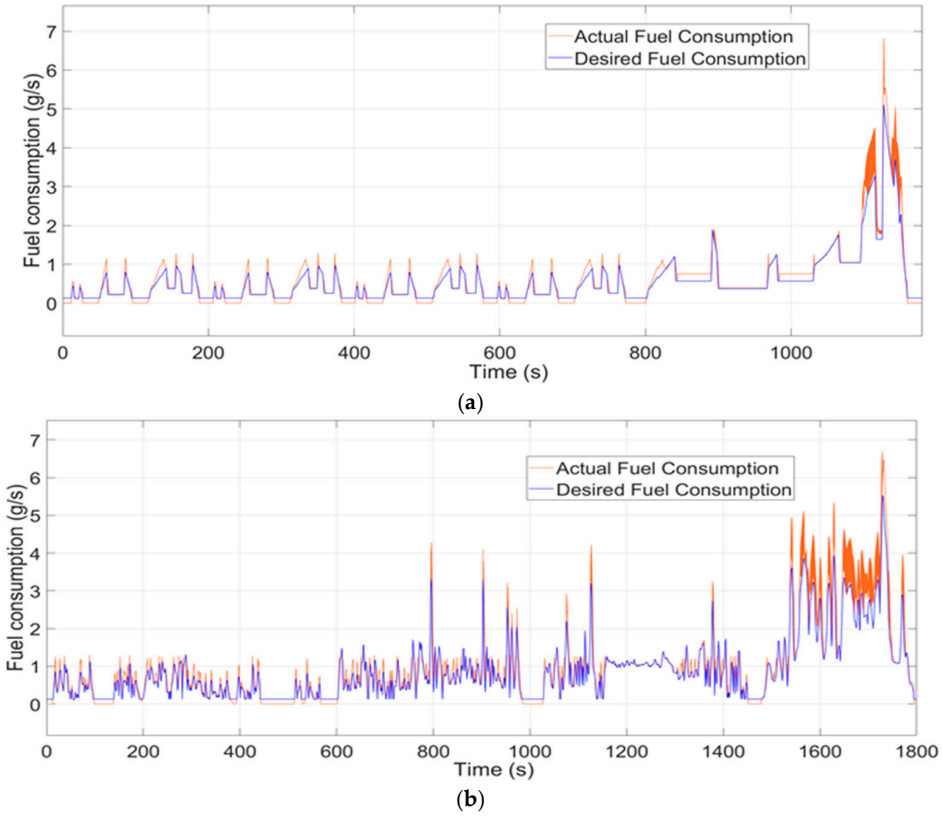


Figure 12. (**a**) Actual and desired fuel consumption for NEDC; (**b**) actual and desired fuel consumption for WLTP.

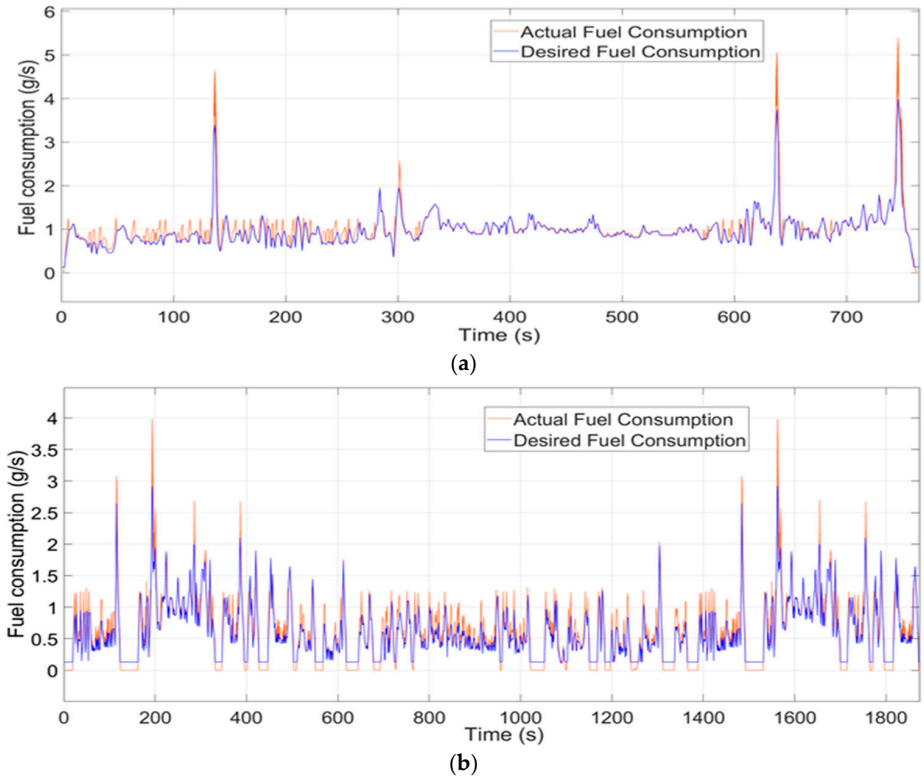


Figure 13. (**a**) Actual and desired fuel consumption for HWFET; (**b**) actual and desired fuel consumption for FTP-75.

The reason for not achieving 0.95–1 R-squared values is due to dimensional boundaries. Theoretically, a gearbox can be designed for all road conditions by increasing gear dimensions, but this would result in a larger gearbox, higher friction rates, and increased vehicle weight, which is why increasing gear ratios infinitely is impossible. Multiple PID variants are applied, but analysis is interrupted when the gear ratio reaches five, as it exceeds the common passenger car gear ratio, as explained above.

In the study, the gear ratio (i_d) is limited to five to keep results applicable to real life. Independently, found fuel consumption values are compatible with the literature [4,26] since the fuel consumption of NEDC is lower than WLTP, since WLTP is a relatively more aggressive cycle, as explained in Section 2.2.

In Figure 10, for NEDC and WLTP cycles, respectively, gear ratio (i_d) values are given.

In Figure 11, for HWFET and FTP-75 cycles, respectively, gear ratio (i_d) values are given.

Figures 12 and 13, NEDC, WLTP, HWFET, and FTP-75, respectively, are given actual and desired fuel consumption graphics. These are also related to R-squared values.

4. Conclusions

In this study, the most appropriate gear ratio values are determined based on the tracking of actual (backward vehicle simulation's fuel consumption, common driving cycles) and desired (minimum fuel consumption) fuel consumption. The obtained results are below:

1. The most appropriate variable gear ratios can be defined by considering the minimum fuel consumption curve, but this gear ratio definition is restricted by limitations, which are based on vehicle weight, dimensions, and the internal friction of the gearbox; however, high R-squared values are accomplished values with basic control after performing various PID configurations, but are only presented the highest R-squared based on gear ratio restriction with basic control.
2. The most appropriate gear ratios are given in Figures 10 and 11 for the most common driving cycles (NEDC, WLTP, HWFET, FTP-75), which represent almost real-life conditions. The most appropriate gear ratio can be determined for any vehicle by calculating the average of these values based on a continuous variable transmission.
3. Obtaining the minimum fuel consumption curve is clearly explained, and dynamic fuel conversion efficiency is used instead of a constant value like others; thus, more accuracy is obtained.
4. The more practical and applicable solution can be produced in real life with PID control without focusing on the purely inner structure of the gearbox. Instead, only gear ratios can be defined by eliminating complexity. In practice, even though CVT is often referred to as having an infinite gear ratio as its advantages, it also presents challenges due to issues related to oil pressure/oil temperature and inner friction/warming.

Author Contributions: All authors contributed to the conception, design, and writing of the manuscript. Authors M.İ.K. and U.C.Ç. were responsible for data collection and analysis, while authors M.İ.K. and U.C.Ç. contributed to the literature review and discussion section. Each author made significant contributions to the development of the research idea and the interpretation of results. All authors have read and agreed to the published version of the manuscript.

Funding: This research received no specific grant from any funding agency in the public, commercial, or not-for-profit sectors.

Data Availability Statement: The data presented in this study are available from the corresponding author upon reasonable request.

Conflicts of Interest: The authors declare that there are no financial contributions or other potential conflict of interest that should be known about the objectivity of the study.

Nomenclature

Road friction coefficient	$C_{rolling}$	Wheel power	P_w
Gravity acceleration	ga	Friction power	P_{R-F}
Mass	m	R-squared	R
Vehicle speed	v_t	Drag power	P_{Drag}
Second	s	Acceleration power	P_a
Drag coefficient	C_{drag}	Engine power	P_e
Projected area	A_p	Engine torque	M_e
Air density	d	Engine radial velocity	W_e
Wheel radius	R_r	Engine revolution per minute	n_e
Differential ratio	i_d	Mass flow rate of fuel	$\dot{m}_f$
Gear ratio	i_g	Extra urban driving cycle	EUDC
Powertrain efficiency	η_a	Brake specific fuel consumption	b_s
The heating value of fuel	Q_{HV}	Fuel conversion efficiency	η_f
Mass of fuel	m_f	Minimum fuel consumption curve	MFCC
Artificial neural network	ANN	All resistance power	P_r
The density of gasoline	d_f	Distance of the related driving cycle	DR
Direct shift gearbox	DSG	New European Driving Cycle	NEDC
Federal test procedure	FTP-75	Continuous variable transmission	CVT
Proportional–integral–derivative	PID	Highway fuel economy test driving	HWFET
Liter	L	Worldwide harmonized light vehicle test procedure	WLTP
Gram	g	Kilometer	Km
Dynamic programming	DP	Energy management system	EMS
One-dimensional	1-D	Urban driving cycle	ECE-15
Environmental protection agency	EPA		

References

1. Gupta, N.; Ram, S. Vehicular Pollution Modeling: Comparative Analysis of CALINE and ANN based pollution models. *Transp. Res. Procedia* **2025**, *82*, 1325–1334. [CrossRef]
2. Bagheri, E.; Tehrani, M.M.; Azadi, M.; Moosavian, A. Impact of driving characteristic parameters and vehicle type on fuel consumption and emissions performance over real driving cycles. *PLoS ONE* **2025**, *20*, e0317098. [CrossRef]
3. Tan, D.; Tan, J.; Liu, M.; Xu, H.; Ge, Y. A combined vehicle specific power and laboratory emissions approach to real driving CO_2 emission estimation for light-duty vehicle. *Sustain. Energy Technol. Assess.* **2025**, *75*, 104265. [CrossRef]
4. Xu, N.; Liu, Q.; Zhang, Z.; Li, J. Development of multiple driving cycles with Equivalent energy consumption to expand a standard driving cycle. *Energy* **2025**, *319*, 134951. [CrossRef]
5. Alatawneh, A.; Torok, A. Projecting AV sales in the EU-27 and UK: Insights from Euro emission standards and historical trends. *Transp. Policy* **2025**, *163*, 91–101. [CrossRef]
6. Williams, M.; Minjares, R. A Technical Summary of Euro 6/VI Vehicle Emission Standards. 2016. Available online: https://www.ccacoalition.org/resources/technical-summary-euro-6vi-vehicle-emission-standards (accessed on 23 November 2025).
7. Zacharof, N.; Broekaert, S.; Grigoratos, T.; Bitsanis, E.; Fontaras, G. A real world assessment of European medium-duty vehicle emissions and fuel consumption. *Atmos. Environ. X* **2025**, *25*, 100307. [CrossRef]
8. Regulation (EC) No 715/2007 on Type Approval of Motor Vehicles. Available online: https://eur-lex.europa.eu/LexUriServ/LexUriServ.do?uri=OJ:L:2007:171:0001:0016:EN:PDF (accessed on 10 August 2020).
9. Pandian, S.; Palanivelu, A. An efficient energy management of a hybrid electric vehicle using hybrid QNN-GOA technique. *J. Energy Storage* **2025**, *106*, 114827. [CrossRef]
10. Ke, T.; Nie, L.; Kecskeméthy, A. Powertrain configuration design for two mode power split hybrid electric vehicle. *Sci. Rep.* **2025**, *15*, 3676. [CrossRef] [PubMed]
11. Zhang, Y.; Yang, Y.; Zou, Y.; Liu, C. Powertrain optimization and performance analysis of series-parallel hybrid transmissions with clutches and gears. *IEEE Trans. Transp. Electrif.* **2025**, *11*, 7859–7873. [CrossRef]

12. Morales, F.; Romero, L.; Benitez, F. Behaviour analysis and general consideration for optimizing Inertial Continuous Variable Transmissions. *Mech. Mach. Theory* **2025**, *206*, 105918. [CrossRef]
13. Wu, S.; Li, C.; Jin, Y.; Zhao, X.; Zhang, J. Energy Saving Design of Gear Hobbing Machine Based on Analytical Target Cascading: Modeling, Decomposition, and Independent Optimization. *IEEE Trans. Autom. Sci. Eng.* **2025**, *22*, 12033–12046. [CrossRef]
14. Zhu, Z.; Hou, R.; Zhang, H.; Wang, D.; Chen, L. Multi-objective optimization of design parameters for tractor hydro-mechanical continuously variable transmissions. *Sci. Rep.* **2025**, *15*, 1–12. [CrossRef]
15. Onori, S.; Serrao, L.; Rizzoni, G. *Hybrid Electric Vehicles Energy Management Strategies*; Springer: London, UK, 2016; p. 3.
16. Naranjo, J.E.; Sotelo, M.A.; Gonzalez, C.; Garcia, R.; Pedro, T. Using Fuzzy Logic in Automated Vehicle Control. *IEEE Intell. Syst.* **2007**, *22*, 36–45. [CrossRef]
17. Li, Y.; Tao, J.; Xie, L.; Zhang, R.; Ma, L.; Qiao, Z. Enhanced Q-learning for real-time hybrid electric vehicle energy management with deterministic rule. *Meas. Control.* **2020**, *53*, 1493–1503. [CrossRef]
18. Bellman, R. *Dynamic Programming*; Princeton University Press: Princeton, NJ, USA, 1957.
19. Fayyazi, M.; Abdoos, M.; Phan, D.; Golafrouz, M.; Jalili, M.; Jazar, R.N.; Langari, R.; Khayyam, H. Real-Time Self-Adaptive Q-Learning Controller for Energy Management of Conventional Autonomous Vehicles. *Expert Syst. Appl.* **2023**, *222*, 119770. [CrossRef]
20. Xia, C.; DU, Z.; Zhang, C. A single-degree-of-freedom energy optimization strategy for power-split hybrid electric vehicles. *Energies* **2017**, *10*, 896. [CrossRef]
21. Phan, D.; Bab-Hadiashar, A.; Lai, C.Y.; Crawford, B.; Hoseinnezhad, R.; Jazar, R.N.; Khayyam, H. Intelligent energy management system for conventional autonomous vehicles. *Energy* **2020**, *191*, 5344. [CrossRef]
22. Tabacu, S.; Popa, D. Backward-Facing Analysis for the Preliminary Estimation of the Vehicle Fuel Consumption. *Sustainability* **2023**, *15*, 5344. [CrossRef]
23. Phan, D.; Bab-Hadiashar, A.; Hoseinnezhad, R.; Jazar, R.N.; Date, A.; Jamali, A.; Pham, D.B.; Khayyam, H. Neuro-fuzzy system for energy management of conventional autonomous vehicles. *Energies* **2020**, *13*, 1745. [CrossRef]
24. Çilingiroğlu, U.C.; Dönmez, M.; Karamangil, M.I. Numerical study of the effect of distance between two light commercial vehicles in convoy on fuel consumption. Uludağ Univ. *J. Fac. Eng.* **2024**, *29*, 37–50. [CrossRef]
25. Gillespie, T.D. *Fundamentals of Vehicle Dynamics*; SAE International: New York, NY, USA, 1992. [CrossRef]
26. Karamangil, M.I.; Tekin, M. Comparison of fuel consumption and recoverable energy according to NEDC and WLTP cycles of a vehicle. *CTF Cienc. Tecnol. Futuro* **2022**, *12*, 31–38. [CrossRef]
27. dos Reis, G.; Strange, C.; Yadav, M.; Li, S. Lithium-ion battery data and where to find it. *Energy AI* **2021**, *5*, 100081. [CrossRef]
28. Zhang, J.; Liggio, J.; Chan, T.W.; Huang, L.; Brook, J.R. Gasoline Direct Injection Engine Emissions of OC and EC: Laboratory Comparisons with Port Fuel Injection Engine. *Aerosol Air Qual. Res.* **2022**, *22*, 220032. [CrossRef]
29. Phan, D.; Amani, A.M.; Mola, M.; Rezaei, A.A.; Fayyazi, M.; Jalili, M.; Pham, D.B.; Langari, R.; Khayyam, H. Cascade adaptive mpc with type 2 fuzzy system for safety and energy management in autonomous vehicles: A sustainable approach for future of transportation. *Sustainability* **2021**, *13*, 10113. [CrossRef]
30. Pulkrabek, W.W. *Engineering Fundamentals of the Internal Combustion Engine*; Pearson Prentice Hall: Hoboken, NJ, USA, 2014.
31. Ozili, P.K. *The Acceptable R-Square in Empirical Modeling for Social Science Research*; IGI Global: Hershey, PA, USA, 2023.
32. Chicco, D.; Warrens, M.J.; Jurman, G. The coefficient of determination R-squared is more informative than SMAPE, MAE, MAPE, MSE and RMSE in regression analysis evaluation. *PeerJ Comput. Sci.* **2021**, *7*, e623. [CrossRef]

Disclaimer/Publisher's Note: The statements, opinions and data contained in all publications are solely those of the individual author(s) and contributor(s) and not of MDPI and/or the editor(s). MDPI and/or the editor(s) disclaim responsibility for any injury to people or property resulting from any ideas, methods, instructions or products referred to in the content.